

## WWER RADIAL REFLECTOR MODELING BY DIFFUSION CODES

P. T. Petkov, Institute for Nuclear Research and Nuclear Energy, Sofia, Bulgaria

S. Mittag, Forschungszentrum Rossendorf, Dresden, Germany

### ABSTRACT

The two commonly used approaches to describe the WWER radial reflectors in diffusion codes, by albedos on the core-reflector boundary and by a ring of diffusive assembly size nodes, are discussed. The advantages and disadvantages of the first approach are presented first, then the Koebke's equivalence theory is outlined and its implementation for the WWER radial reflectors is discussed. Results for the WWER-1000 reactor are presented. Then the boundary conditions on the outer reflector boundary are discussed. The possibility to divide the library into fuel assembly and reflector parts and to generate each library by a separate code package is discussed. Finally, the homogenization errors for rodded assemblies are presented and discussed.

# 1 Introduction

Most part of a PWR (with square assemblies) radial reflector can be modeled in one-dimensional plane geometry with some problems around the core corners. This permits the usage of one-dimensional  $S_N$  transport codes to calculate albedos on the core-reflector boundary or effective few-group diffusion parameters for the reflector nodes. At the same time the few-group flux modeling within the reflector nodes is very simple. Thus, the PWR radial reflector modeling poses no severe problems.

The WWER radial reflectors are much more complicated due to the hexagonal shape of the fuel assemblies. The WWER-1000 radial reflector is presented on Figure 1. The shadings represent stainless steel, the rest being coolant. A two-dimensional transport theory code is required to solve the neutron transport equation for the core and radial reflector in order to calculate albedos on the core-reflector boundary or effective few-group diffusion parameters for the reflector. Moreover, the few-group flux distribution within the homogenized reflector nodes is also very complicated.

The complicated nature of the WWER radial reflectors is the main reason that all three-dimensional diffusion codes, designed for steady-state neutronics calculations of the WWER reactors, use albedo-type boundary conditions on the core-reflector boundary. The albedos are not easier to calculate, but they are easily fitted. The SPPS-1.6 [1] library of two-group diffusion parameters for WWER-440, generated in 1995, was equipped with albedo boundary conditions, estimated by the 1D transport theory code ANISN [2] and fitted to experimental data. The fitting procedure is rather an art problem than a scientific one. The fitting parameters (correction factors) depend on the person doing the fitting. It takes a lot of time and is prone to uncertainties. The fitting is based on the assembly-wise power distributions, available only for full-power states. There is no guarantee that the fitting parameters will be valid for low-temperature states or for high-temperature and low-density states, occurring in accident analysis. Moreover, systematic errors in the experimental data can be included in the calculational results.

The transport theory code Mariko [3, 4, 5], based on the method of characteristics and with explicit treatment of the scattering anisotropy, has been capable of solving two-dimensional heterogeneous full core problems since 2001, thanks to the progress in PC performance. An algorithm for calculation of accurate albedos on the core-reflector boundary has been included in Mariko [6]. But the possibility to calculate accurate albedos revealed the disadvantage of the conventional group to group albedos,  $\alpha_{h \leftarrow g}$ , which assume that the partial in-current on an outer node face depends only on the partial out-currents on the same node face, thus neglecting neutron transfer through the reflector from one outer node face to another. In other words, the conventional group to group albedos depend essentially on the fuel loading on the core periphery (more precisely, on the flux distribution near the radial reflector). This was the reason to develop an algorithm for calculation of face-group to face-group albedos,  $\alpha_{jh \leftarrow ig}$  (the probability that a neutron leaving the core from outer node face  $i$  in group  $g$  will return back to the core through outer node face  $j$  in group  $h$ ). Since Mariko is a 2D code, only neutron transfer in the horizontal plane was considered. The library of such albedos, calculated in 2001, was included in the SPPS-1.6 library [7] and later in the SPPS-2 library [8]. Comparison to experimental data showed no need to fit the radial reflector albedos for full core, but in case of reduced core a 5% reduction of  $\alpha_{1 \leftarrow 1}$  was needed.

It is natural to suggest that if the neutron transfer between outer node faces is essential in the radial plane, it will be essential also in the axial direction. Test calculations by Mariko showed that in case of small axial node size (12 cm) the axial neutron transfer between neighbor nodes through the radial reflector is about 40% of the returning fast neutrons. The same should be true for the WWER-440 control absorber. But it is very difficult to calculate 3D albedos by a 2D code, and 3D calculations cannot be performed by now.

Another disadvantage of the albedo-type boundary conditions is the assumption that they are constant on an outer node face. This assumption leads to significant errors in the pin-wise power distribution near the core-reflector boundary [9]. The errors can be reduced to tolerable limits if the variation of the albedos along the outer assembly face is taken into account [10].

The above described disadvantages of the albedo-type boundary conditions could be avoided if the radial reflector is described by diffusive nodes. The axial and radial neutron transfer within the reflector is described explicitly, although in diffusion approximation, while the interaction of the outer fuel nodes with radial reflector nodes should be much more natural (close to the real one). However, the calculation of effective diffusion parameters for the radial reflector nodes is not a trivial problem.

## 2 The Koebke's equivalence theory

The Koebke's equivalence theory (ET) [11, 12, 13] has been developed in order to define equivalent homogenized few-group diffusion parameters for a region, which should preserve both the region-averaged reaction rates and the face-averaged net currents, corresponding to an accurate many-group heterogeneous solution. This can be achieved for any approximate method used to solve the few-group diffusion equation, but the equivalent homogenized few-group diffusion parameters are specific for each method (see section 3 in [13]).

The Koebke's ET suggests that a many-group heterogeneous solution is available inside the region to be homogenized and at least one mean free path away from it. This condition is almost fully met by the many-group heterogeneous full core transport solution by Mariko. The term almost is used because the peripheral fuel assemblies can be quite different, therefore the flux distribution around the core-reflector boundary can be quite different as well, and the sensitivity of the equivalent homogenized few-group diffusion parameters to the fuel loading on the core periphery must be studied.

Postulate A in Ref. [11] states that the integral reaction rates and fluxes of the many-group heterogeneous solution should be preserved in every homogenized region (in our case in each reflector node) and for any macrogroup.

The Mariko code solves the neutron transport equation for a 30- or 60-degree sector of the core and radial reflector. The domain of solution is divided into macrocells (a fuel assembly is a macrocell and a reflector node is a macrocell, too), the macrocells are divided into cells (a fuel cell is a cell), and the cells are divided into regions, the material in each region being described by spatially constant macroscopic cross sections. The many-group solution by Mariko provides scalar fluxes  $\phi_{ig}$  by region  $i$  and group  $g$ . The macrocell-averaged few-group fluxes and cross sections are calculated by the conventional formulas for homogenization and condensation:

$$\phi_{IG} = \frac{\sum_{i \in I} \sum_{g \in G} \phi_{ig} a_i}{A_I},$$

$$\Sigma_{IG}^x = \frac{\sum_{i \in I} \sum_{g \in G} \Sigma_{i,g}^x \phi_{ig} a_i}{\phi_{IG} A_I},$$

where  $\sum_{i \in I}$  means summation over all regions  $i$  in macrocell  $I$ ,  $\sum_{g \in G}$  means summation over all groups  $g$  in macrogroup  $G$ , and  $a_i$  and  $A_I$  are the region and macrocell areas. Also the conventional formula for calculation of scattering cross sections is applied. Thus, with the conventional definitions of the few-group macroscopic cross sections, postulate A will be fulfilled if the node-averaged few-group fluxes are preserved.

The diffusion coefficient is always a special problem. The  $B_1$  method, conventionally applied for calculation of diffusion coefficients in case of single fuel assembly calculations, is not applicable for non-multiplying regions. There are two extreme cases for condensation of the

diffusion coefficient—by flux averaging of  $\frac{1}{\Sigma^{\text{tr}}}$  or  $\Sigma^{\text{tr}}$ . Numerical tests showed that the following combination of these two is very close to the  $B_1$  diffusion coefficients in case of single fuel assembly calculations:

$$D_{IG} = \frac{1}{3(3\Sigma_{1IG}^{\text{tr}} + \Sigma_{2IG}^{\text{tr}})/4},$$

where

$$\Sigma_{1IG}^{\text{tr}} = \frac{\phi_{IG}}{\sum_{g \in G} \frac{A_I \phi_{Ig}^2}{\sum_{i \in I} \Sigma_{ig}^{\text{tr}} \phi_{ig} a_i}},$$

$$\Sigma_{2IG}^{\text{tr}} = \frac{\sum_{g \in G} \sum_{i \in I} \Sigma_{ig}^{\text{tr}} \phi_{ig} a_i}{\phi_{IG} A_I},$$

and  $\phi_{Ig}$  is the macrocell-averaged flux in group  $g$ . These diffusion coefficients are calculated for the reflector macrocells or nodes.

Postulate B in Ref. [11] states that the integral net currents and the integral fluxes should be preserved at the interfaces between adjacent regions, in our case on the radial reflector node faces (sides), for each macrogroup. In order to satisfy both postulates, Koebke defines an inhomogeneous boundary value problem for each region to be homogenized. The few-group flux solution of the homogenized problem must preserve the node-averaged fluxes and the face-averaged net currents, but in general this solution will not preserve the face-averaged fluxes. Defining for each group and each node face the heterogeneity factor as the ratio of the heterogeneous face-averaged flux to the homogeneous (obtained by solving the inhomogeneous boundary value problem) face-averaged flux,

$$f = \frac{\phi^{\text{het}}}{\phi^{\text{hom}}},$$

the conventional flux continuity condition is replaced by the requirement that the face-averaged flux times the heterogeneity factor be continuous. Thus, postulate B is met with a different sense for the face-averaged fluxes.

Koebke considered also the possibility to determine better values for the diffusion coefficients, while Smith [13] fixed the diffusion coefficients (to the ones condensed by flux averaging of  $\frac{1}{\Sigma^{\text{tr}}}$ ) and named the resulting heterogeneity factors reference discontinuity factors (RDFs). The RDFs compensate the errors due to: replacement of the real heterogeneous structure with homogeneous one; few-group approximation; diffusion approximation; approximate method to solve the few-group diffusion equation.

The following is a possible implementation of the Koebke's ET. The Mariko code calculates the partial currents on each region edge for each group. From these a special algorithm calculates the partial currents for each cell side, lying on macrocell faces. From these in turn the average partial currents  $j_{ILG}^{\pm}$  by macrocell  $I$ , face  $L$ , and macro-group  $G$  can be calculated. These partial currents are used to calculate the macrocell face-averaged fluxes  $\phi_{ILG}$  and net currents  $J_{ILG}$ .

For macrocell  $I$  the inhomogeneous boundary value problem is defined as follows:

- the conventional few-group diffusion equation is valid within the macrocell with the above defined homogenized diffusion parameters (including the diffusion coefficients);
- the net currents  $J_{ILG}$  are used as boundary conditions on all faces  $L$  of macrocell  $I$  for macrogroup  $G$ .

From the solution of this inhomogeneous boundary value problem, the face-averaged homogeneous fluxes,  $\phi_{ILG}^h$ , can be calculated and the reference discontinuity factors are obtained:

$$f_{ILG} = \frac{\phi_{ILG}}{\phi_{ILG}^h}.$$

If the inhomogeneous boundary value problem is solved exactly, e.g. by the finite-difference method with very fine meshes, then unique RDFs will be obtained. But the real few-group flux distribution within the homogenized reflector nodes is too complicated for the flux modeling in the nodal diffusion codes. If the flux modeling of a particular nodal method is used to solve the inhomogeneous boundary value problem, then the resulting RDFs will compensate also the errors due to the flux modeling by this particular nodal method. Thus, the RDFs will be different for each nodal method.

The Koebke's ET is applicable also for the axial reflectors, for which one-dimensional modeling is sufficient.

### 3 Application of the Koebke's equivalence theory

The application of the Koebke's ET for the WWER-440 reactors has been described in Ref. [14]. It must be noted that this implementation does not take full advantage of the Koebke's ET, because the flux modeling used to solve the inhomogeneous boundary value problem does not coincide with the HEXNEM1 method implemented in DYN3D [15]. Nevertheless, the results are very good and the reflector modeling by diffusive nodes proved to be equivalent to core-reflector albedos. It has been demonstrated, that the RDFs are insensitive to the fuel loading on the core periphery.

In this report similar results are presented for the WWER-1000 reactor. The same procedure for calculation of RDFs has been used, although this time the HEXNEM2 method, which requires both side and corner RDFs, has been used in DYN3D.

The reference solution is for the first two-dimensional heterogeneous transport theory hot zero-power benchmark for the WWER-1000 reactors [16] with all control clusters up. The results by DYN3D with unity discontinuity factors (UDFs) both for the fuel assemblies and the radial reflector nodes are compared to the reference solution on Fig. 2. The errors in the relative assembly-wise power distribution vary between -9.0% and +11.5%. The application of assembly discontinuity factors (ADFs) for the fuel assemblies, but with UDFs for the radial reflector nodes, decreases the errors (Fig. 3) and now they vary between -6.2% and +6.7%. The application of RDFs for the radial reflector nodes (Fig. 4) further decreases the errors and now they range between -2.0 and +2.1. If group to group albedos, calculated specifically for this problem, are used on the core-reflector boundary (Fig. 5), the errors vary between -0.9% and +1.5%. It should be noted, that the HEXNEM2 method requires corner albedos on the core-reflector boundary, which had not been calculated and the corresponding side albedos are used.

### 4 Conditions on the outer reflector boundary

Usually one ring of radial reflector nodes is used to describe the radial reflector in nodal diffusion codes and albedo-type boundary conditions are applied on the outer boundary of the radial reflector nodes. In the current version of DYN3D these albedos are not parameterized (they are constant), which may cause problems. We know from the reactor physics books that a 20 cm radial reflector is thick enough, i.e. the boundary conditions applied on the outer boundary of such reflector do not affect  $k_{\text{eff}}$  and the flux solution inside the core. However, this is true for a water reflector at room temperature. In case of steel reflector the corresponding thickness is

40-45 cm, because the steel mainly scatters the fast neutrons without significant energy loss and they travel longer distances. If the coolant density is low, then the reflector thickness should be more than 20 cm even for water reflectors. It is not convenient to add additional rings of reflector nodes and the calculation of RDFs for the additional nodes may be problematic. A way out of this situation is to use parameterized albedo boundary conditions on the outer boundary of a single ring of reflector nodes, i.e. to regard them as functions of the temperature, moderator density and boron concentration. Appropriate tables of albedo boundary conditions can be calculated by Mariko and parameterized accordingly.

The same considerations are valid for the bottom reflector and especially for the top reflector. In case of coolant boiling the moderator density can be very low and the coolant part of the top reflector will become transparent to the neutrons. The bottom and top reflectors can be described by 20 cm layers and parameterized albedos can be applied on the outer reflector boundaries. In calculating the albedos for the axial reflectors by Mariko it is possible to describe explicitly say 100 cm of the corresponding reflector and the albedos will include the effect of the part of the reflector, not explicitly modeled by the diffusion code.

## 5 Library of diffusion parameters for the reflectors

The effective diffusion parameters for the radial, bottom, and top reflectors, as well as the albedos on the outer reflector boundaries can form a reflector library, which is separate from the library of diffusion and kinetics parameters for the fuel assemblies. It should be separate, because the parameterization of the reflector diffusion parameters can be different from that of the fuel assemblies, and also because it can be calculated by a separate code package. The nuclear data libraries of the present day lattice codes are based on the recent evaluated nuclear data files, in which the cross sections of all isotopes, encountered in the reflectors, are very close. The core loading is not essential when reflectors are calculated. Therefore, any lattice code can be used to prepare the many-group cross sections for the fuel assemblies. For the steel in the reflectors there is a special problem with the self-shielding of the high energy scattering resonances of  $\text{Fe}^{56}$ , which cannot be solved by the lattice codes. Finally, the reflector library can be prepared separately from the fuel assembly library, applying advanced methods.

## 6 The all control clusters down benchmark

The comparison of the relative assembly-wise power distribution by DYN3D and the reference Mariko solution for the last benchmark in Ref. [16] with all control rods down is presented on Fig. 6. The errors are quite big, but the reason is neither in the reflector modeling, nor in the HEXNEM2 method (both ADFs and RDFs are taken into account), but in the homogenization. In the DYN3D calculation asymptotic diffusion parameters are used for each assembly type, obtained from single assembly calculations assuming an infinite array of identical assemblies. In the full-core Mariko calculation 23 group cross sections are used, separate for each fuel pin, each cladding, and the moderator in each cell (also obtained by single assembly calculations). Thus, the real environment of the assembly is simulated. Using these cross sections and the region-averaged fluxes from the full-core Mariko solution, real two-group macroscopic cross sections can be calculated for each fuel assembly. The real and asymptotic two-group cross sections are compared on Table 1. The effect on  $k_\infty$  of the deviations is also presented.

The biggest error on Fig. 6 is in assembly 1. It is a 3.0% rodded assembly, surrounded by six 1.6% assemblies. The net deviation of the real  $k_\infty$  value from the asymptotic one is 1412 pcm, the main contribution coming from the thermal capture (756 pcm). The reason can be understood by the following considerations. The thermal flux level in the central 3.0% assembly is lower than the level in the surrounding six 1.6% assemblies, which results in thermal neutron

transfer to the 3.0% assembly through its faces. This effect is described by the transient mode in the modal nodal methods. But the diffusion length of the thermal neutrons is only about 2 cm and they can hardly reach the absorber rods in the 3.0% assembly, which are more than 4 cm away from the assembly faces. Thus, for the transient neutron flux the cross sections of the central assembly are quite different from the assembly averaged ones, containing the smeared control rod absorbers. Similar deviations in  $k_{\infty}$  are observed for assemblies 8 and 15, which are 3.0% rodded assemblies, each one surrounded by four 1.6% assemblies and two 3.0% assemblies.

A solution for this problem can be the introduction of separate cross sections for the transient and fundamental mode fluxes, but a special study is required anyway.

The above results demonstrate the advantages of the transport theory benchmarks. They can be regarded as ideal experiments and permit the assessment of the errors due to the homogenization, few-group diffusion approximation, and the flux modeling by the nodal methods. The diffusion equation is a crude approximation to the neutron transport equation, the homogenization and condensation errors can be very big, especially in kinetics calculations, but almost all available benchmarks are for normal operational conditions. In case of kinetics calculations the range of core states is much wider and new benchmarks are needed. Transport theory benchmarks can be stated for low-temperature high-density states, high-temperature low-density states, coolant boiling in an assembly, and many other core states, typical for kinetics calculations.

## References

- [1] P. T. Petkov. “*SPPS-1.6 - A 3D Diffusion Code for Neutronics Calculations of the WWER-440 Reactors*”. Proc. IV AER Symposium, Sozopol, Bulgaria, (1994)
- [2] D. Kent Parsons. “*ANISN/PC Manual*”. EGG-2500, April (1987)
- [3] P. T. Petkov, T. Takeda. “*Transport Calculations Of MOX and UO<sub>2</sub> Pin Cells by the Method of Characteristics*”. JNST, Vol. 35, No. 12, pp. 874-885 (1998)
- [4] P. T. Petkov, T. Takeda. “*Comparison of the Flat and Linear Source Variants of the Method of Characteristics*”. ANE, Vol. 26, pp. 935-942 (1999)
- [5] P. T. Petkov. “*Development of a Neutron Transport Code for Many-Group Two-Dimensional Heterogeneous Calculations by the Method of Characteristics*”. Proc. X AER Symposium, Moscow, Russia, 271-280 (2000)
- [6] P. T. Petkov. “*Calculation of Accurate Albedo Boundary Conditions for Three-Dimensional Nodal Diffusion Codes by the Method of Characteristics.*”, Proc. X AER Symposium, Moscow, Russia, 407-418 (2000)
- [7] P. T. Petkov, Tz. Haralampieva, T. Simeonov, I. Stoyanova, K. Kamenov. “*Generation of a library of two-group diffusion parameters for SPPS-1.6 by HELIOS*”. Proc. X AER Symposium, Moscow, Russia, 259-270 (2000)
- [8] P. T. Petkov, I. D. Christoskov, I. Stoyanova, K. Kamenov, A. Tomov. “*A New Version of the SPPS In-Core Fuel Management Code Package for the WWER-440 Reactors*”. Proc. XIII AER Symposium, Dresden, Germany, 287-298 (2003)
- [9] P. T. Petkov, Tz. Haralampieva, K. Kamenov. “*Validation of a two-group two-dimensional fine-mesh neutron diffusion code for calculation of the pin power peaking factors in the WWER-440 cores*”. Proc. XI AER Symposium, Chopak, Hungary, 87-106 (2001)

- [10] P. T. Petkov. “*Two-Dimensional Full-Core Transport Theory Benchmarks for the WWER Reactors*”. Proc. XII AER Symposium, Sunny Beach, Bulgaria, 191-204 (2002)
- [11] K. Koebke. “*A New Approach to Homogenization and Group Condensation.*” Lugano, IAEA-TECDOC-231, 1978
- [12] K. Koebke. “*Advances in Homogenization and Dehomogenization.*” Int. Topical Meeting on Advances in Math. Methods for the Solution of Nucl. Eng. Problems, Munich, 1981
- [13] K. S. Smith. “*Assembly Homogenization Techniques for Light Water Reactor Analysis.*” Progress in Nuclear Energy, Vol. 17, No. 3, pp. 303-335, 1986
- [14] S. Mittag, P. T. Petkov, U. Grundman. “*Discontinuity factors for non-multiplying material in two-dimensional hexagonal reactor geometry*”. Annals of Nuclear Energy 30, 1347-1364 (2003)
- [15] U. Grundmann, F. Hollstein. “*A two-dimensional intranodal flux expansion method for hexagonal geometry*”. Nucl. Sci. Eng., 133, 201 (1999)
- [16] P. T. Petkov, S. Mittag. “*Two-Dimensional Heterogeneous Transport Theory Hot Zero-Power Benchmarks for the WWER-1000 Reactors*”. Proc. XIII Symposium of AER, Dresden, Germany, 77-88 (2003)

Table 1: Relative deviations [pcm] between the real and asymptotic diffusion parameters and  $k_\infty$  for benchmark BB

n	s	$k_\infty$	$\Sigma_f^c$	$k_\infty$	$\nu\Sigma_f^f$	$k_\infty$	$\Sigma_f^s$	$k_\infty$	$\Sigma_t^c$	$k_\infty$	$\nu\Sigma_t^f$	$k_\infty$
1	4	1412	-1209	382	-25	-3	86	15	-2232	756	745	247
2	1	-181	-379	85	-519	-51	-1269	-162	-245	101	-369	-153
3	3	97	-544	159	143	18	-414	-68	303	-115	220	84
4	2	404	-1902	455	-1359	-144	-792	-107	-922	314	-257	-86
5	3	87	-519	152	138	17	-397	-65	281	-106	189	72
6	1	-222	-261	59	-564	-56	-1229	-157	-291	120	-446	-184
7	5	-111	98	-31	226	35	34	5	496	-173	137	48
8	4	1025	-1136	359	-196	-27	-211	-37	-1641	554	506	168
9	1	-184	-365	82	-522	-52	-1250	-159	-251	104	-379	-157
10	3	87	-485	142	169	21	-360	-59	277	-105	185	70
11	2	275	-1788	428	-1363	-145	-733	-99	-697	237	-348	-116
12	4	298	-925	292	-466	-64	-624	-111	-553	186	4	1
13	6	-427	1625	-530	633	101	1906	313	620	-214	-195	-67
15	4	952	-1043	329	-130	-18	-121	-21	-1487	502	458	152
16	2	205	-1689	404	-1298	-138	-640	-86	-548	186	-396	-133
17	5	-71	-450	145	27	4	-806	-133	496	-173	189	66
18	6	-313	745	-243	326	52	796	131	600	-207	-101	-35
21	4	264	-848	267	-427	-59	-522	-92	-488	164	-27	-9
22	5	-330	677	-218	320	50	553	91	701	-244	11	3



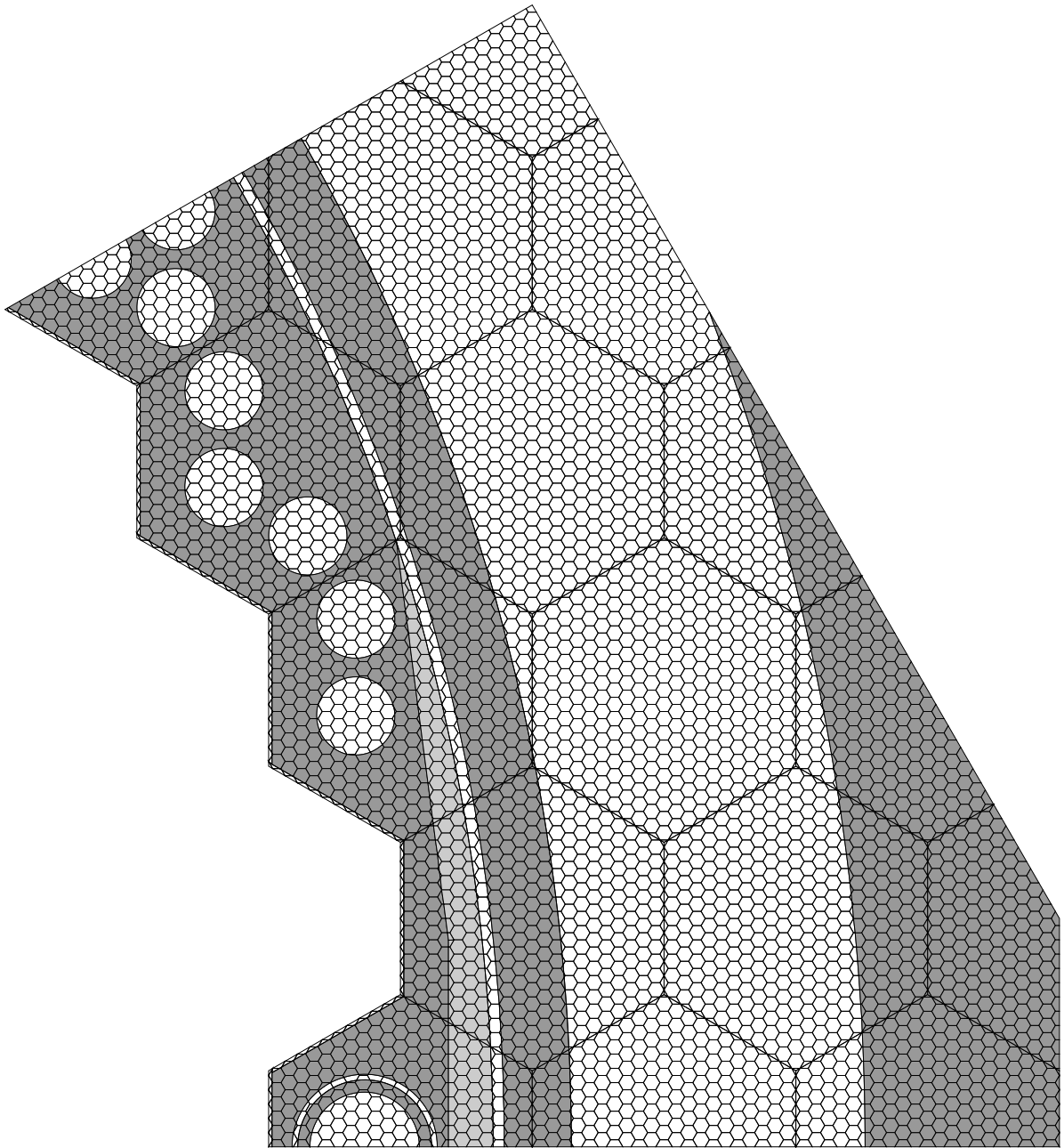


Figure 1: WWER-1000 radial reflector (30 degree sector). The shaded regions represent stainless steel, the lightly shaded region represents a mixture of steel and coolant, and the rest is coolant. The small meshes represent the regions for the heterogeneous transport calculation by Mariko

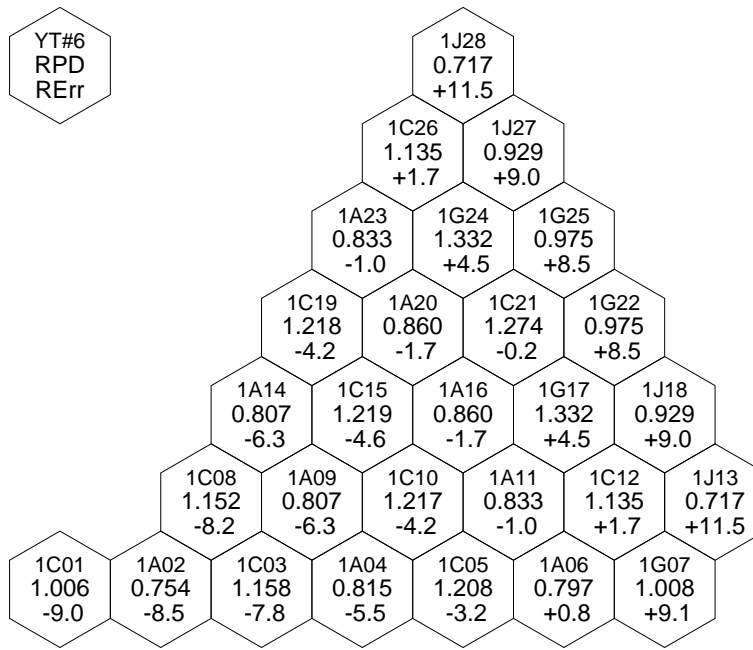


Figure 2: Relative assembly-wise power distribution by DYN3D with assembly UDFs and reflector UDFs and relative deviations [%] from Mariko for benchmark B1.  $k_{\text{eff}}$  error +200 pcm

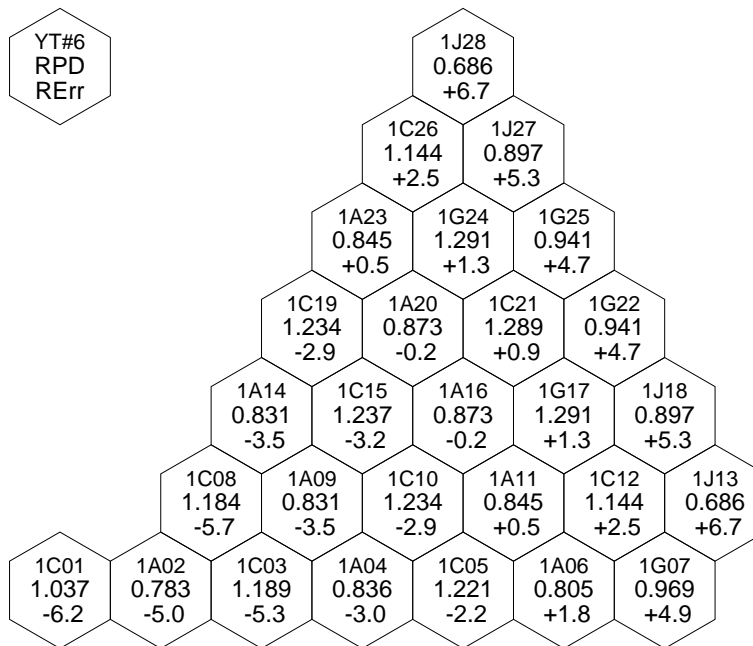


Figure 3: Relative assembly-wise power distribution by DYN3D with assembly ADFs and reflector UDFs and relative deviations [%] from Mariko for benchmark B1.  $k_{\text{eff}}$  error +86 pcm

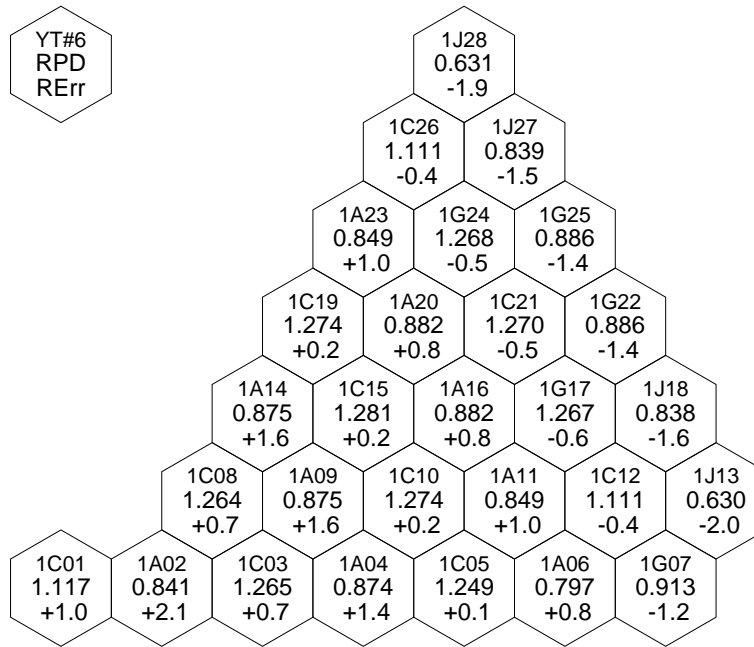


Figure 4: Relative assembly-wise power distribution by DYN3D with assembly ADFs and reflector RDFs and relative deviations [%] from Mariko for benchmark B1.  $k_{\text{eff}}$  error -77 pcm

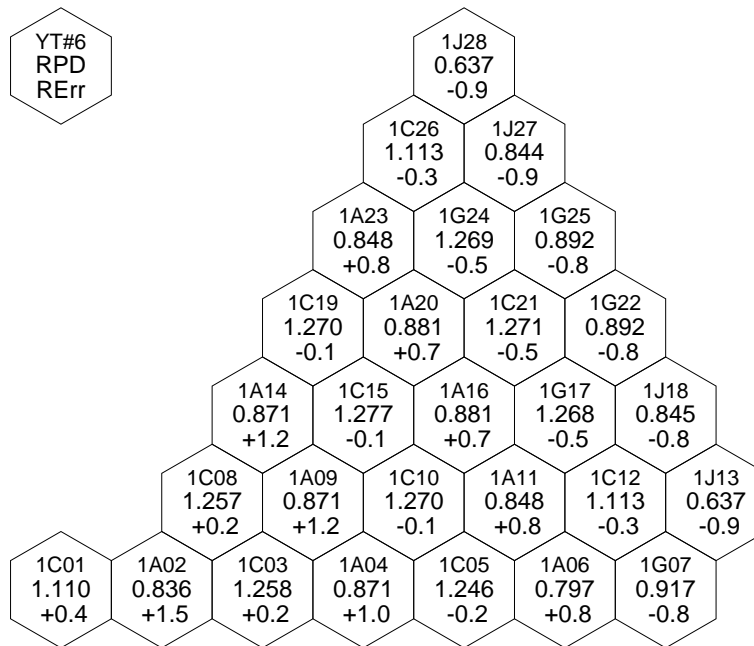


Figure 5: Relative assembly-wise power distribution by DYN3D with assembly ADFs and core-reflector albedos and relative deviations [%] from Mariko for benchmark B1.  $k_{\text{eff}}$  error -62 pcm

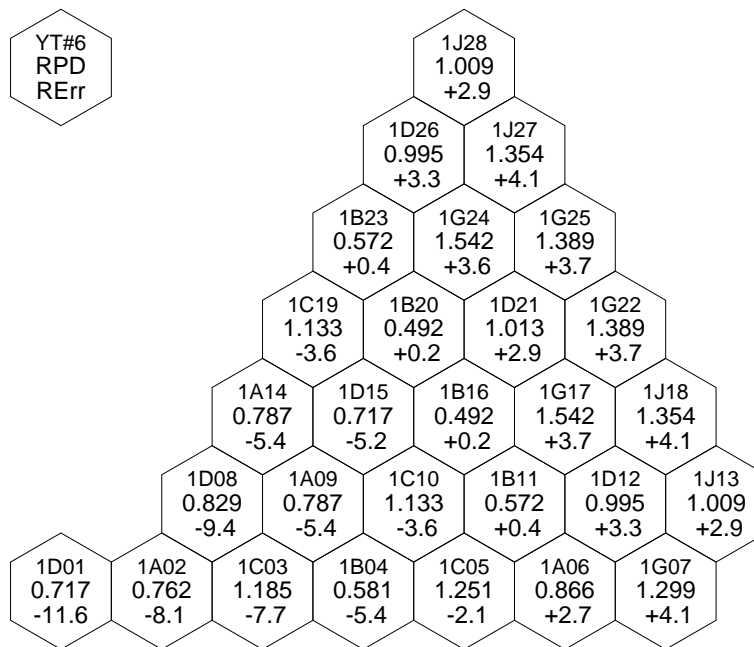


Figure 6: Relative assembly-wise power distribution by DYN3D and relative deviations [%] from Mariko for benchmark BB.  $k_{\text{eff}}$  error -56 pcm